© 2014. Published by The Company of Biologists Ltd | Development (2014) 141, 2885-2894 doi:10.1242/dev.099150

RESEARCH ARTICLE

Dimeric combinations of MafB, cFos and cJun control the apoptosis-survival balance in limb morphogenesis

Natsuno Suda[1], Takehiko Itoh[2], Ryuichiro Nakato[3], Daisuke Shirakawa[1], Masashige Bando[3], Yuki Katou[3], Kohsuke Kataoka[4], Katsuhiko Shirahige[3], Cheryll Tickle[5] and Mikiko Tanaka[1,*]

ABSTRACT

Apoptosis is an important mechanism for sculpting morphology. However, the molecular cascades that control apoptosis in developing limb buds remain largely unclear. Here, we show that MafB was specifically expressed in apoptotic regions of chick limb buds, and MafB/cFos heterodimers repressed apoptosis, whereas MafB/cJun heterodimers promoted apoptosis for sculpting the shape of the limbs. Chromatin immunoprecipitation sequencing in chick limb buds identified potential target genes and regulatory elements controlled by Maf and Jun. Functional analyses revealed that expression of *p63* and *p73*, key components known to arrest the cell cycle, was directly activated by MafB and cJun. Our data suggest that dimeric combinations of MafB, cFos and cJun in developing chick limb buds control the number of apoptotic cells, and that MafB/cJun heterodimers lead to apoptosis via activation of *p63* and *p73*.

KEY WORDS: AP-1 transcription factor, Limb, Chick

INTRODUCTION

During vertebrate development, apoptosis is a crucial process that sculpts the shape of embryos. In this regard, vertebrate limbs provide one of the best models in which to study apoptosis, as it has major morphogenetic functions. In avian limbs, the elimination of cells is observed in four distinct mesenchymal areas: the anterior necrotic zone (ANZ), posterior necrotic zone (PNZ), opaque patch (OP) and interdigital necrotic zones (INZs). In the ectoderm, cells are eliminated in the apical ectodermal ridge (Todt and Fallon, 1986; Zuzarte-Luis and Hurle, 2002). Apoptosis in these regions is particularly important because disruptions in apoptosis affect the final morphology of the limb (Ros et al., 1997; Yokouchi et al., 1996; Zuzarte-Luis and Hurle, 2002). Numerous studies have shown that bone morphological proteins (BMPs) trigger apoptosis both in the mesodermal cells (Ganan et al., 1996; Macias et al., 1997; Tang et al., 2000; Yokouchi et al., 1996; Zou and Niswander, 1996) and in the ectoderm of the apical ectodermal ridge (Wang et al., 2004). Overexpression of a dominant-negative form of BMP receptor Ib or Ia in chick limb represses apoptosis and induces the formation of interdigital webs (Yokouchi et al., 1996; Zou and Niswander, 1996), whereas transplantation of a BMP protein-soaked bead in limb mesenchyme induces apoptosis in chick embryos (Ganan et al., 1996; Macias et al., 1997; Tang et al., 2000). However, the molecular cascades that connect BMP signalling with the expression of genes controlling apoptosis in limbs remain largely unclear.

The AP-1 transcription factor superfamily is well conserved, and its members regulate the transcription of genes involved in diverse cellular processes, including proliferation, transformation and death (Shaulian and Karin, 2002). During vertebrate embryogenesis, some AP-1 transcription factors are crucial for the proper development of bones and the lens, liver and heart (Ogino and Yasuda, 1998; Shaulian and Karin, 2002). AP-1 transcription factors are also known to modulate gene expression triggered by free radicals (Sen and Packer, 1996). Interestingly, high levels of reactive oxygen species (ROS) are present in the INZ, and antioxidants can reduce apoptosis in limb buds (Salas-Vidal et al., 1998; Schnabel et al., 2006), suggesting that ROS stress may trigger apoptosis in the INZ. Indeed, the AP-1 family members cFos and cJun are regulated by oxidants at both transcriptional and translational levels (Sen and Packer, 1996).

Here, we examine the molecular cascades that control apoptosis in developing limb buds and tested the involvement of AP-1 transcription factor members in this process. Global expression profiles of all 41 reported AP-1 superfamily members showed that expression of *MafB* was restricted to the area of apoptosis. Thus, we examined whether MafB, as well as its candidate heterodimer partners cJun and cFos (Deppmann et al., 2006), are involved in controlling apoptosis during limb morphogenesis. Gain- and loss-of-function experiments revealed that MafB/cFos heterodimers inhibited apoptosis, whereas MafB/cJun heterodimers promoted apoptosis for sculpting the shape of chick limb buds. Integrating chromatin immunoprecipitation sequencing (ChIP-Seq) and functional analyses showed that expression of the transcription factors *p63* and *p73* was directly activated by MafB and cJun. Our results suggest that the balance of MafB, cFos and cJun heterodimer combinations controls the number of apoptotic cells and that the MafB/cJun heterodimer triggers pathways that lead to apoptosis via activation of *p63* and *p73* during chick limb morphogenesis.

RESULTS

Global gene expression profiles of AP-1 superfamily members in chick limb buds

In vertebrates, AP-1 superfamily transcription factors are involved in many processes that are crucial to the function of an organism. Some are necessary for the proper development of several organs and tissues (Shaulian and Karin, 2002). We explored whether any genes that encode AP-1 transcription factors are involved in regulating apoptosis in chick limb buds. Expression patterns of genes encoding all 41 AP-1 members that are present in chickens were examined in chick wing buds at stage 26 and in leg buds at

[1]Graduate School of Bioscience and Biotechnology, Tokyo Institute of Technology, B-17, 4259 Nagatsuta-cho, Midori-ku, Yokohama 226-8501, Japan. [2]Graduate School of Bioscience and Biotechnology, Tokyo Institute of Technology, B-34, 4259 Nagatsuta-cho, Midori-ku, Yokohama 226-8501, Japan. [3]Institute of Molecular and Cellular Biosciences, University of Tokyo, 1-1-1 Yayoi, Bunkyo-ku, Tokyo 113-0032, Japan. [4]Graduate School of Medical Life Sciences, Yokohama City University, 1-7-29 Suehiro-cho, Tsurumi-ku, Yokohama 230-0045, Japan. [5]Department of Biology and Biochemistry, University of Bath, Claverton Down Road, Bath BA2 7AY, UK.

*Author for correspondence (mitanaka@bio.titech.ac.jp)

Received 17 May 2013; Accepted 20 May 2014

Development (2014) 141, 2885-2894 doi:10.1242/dev.099150

stage 31 (supplementary material Fig. S1). Of these, *MafB* transcripts were detected in the areas of apoptosis, including the ANZ, the PNZ and the apical ectodermal ridge at stage 26 (Fig. 1A) and the INZ at stage 31 (Fig. 1B), as previously reported (Lecoin et al., 2004). Based on their structural similarities, MafB was predicted to form heterodimers with either Fos or Jun family members (Deppmann et al., 2006). Among all Fos and Jun family members, only *cFos* and *cJun* transcripts were detected throughout the wing and leg buds of chick embryos, including apoptotic regions (Fig. 1C-F; supplementary material Fig. S1). Thus, we next examined whether MafB and its candidate heterodimer partners cFos and cJun were involved in regulating apoptosis during limb morphogenesis.

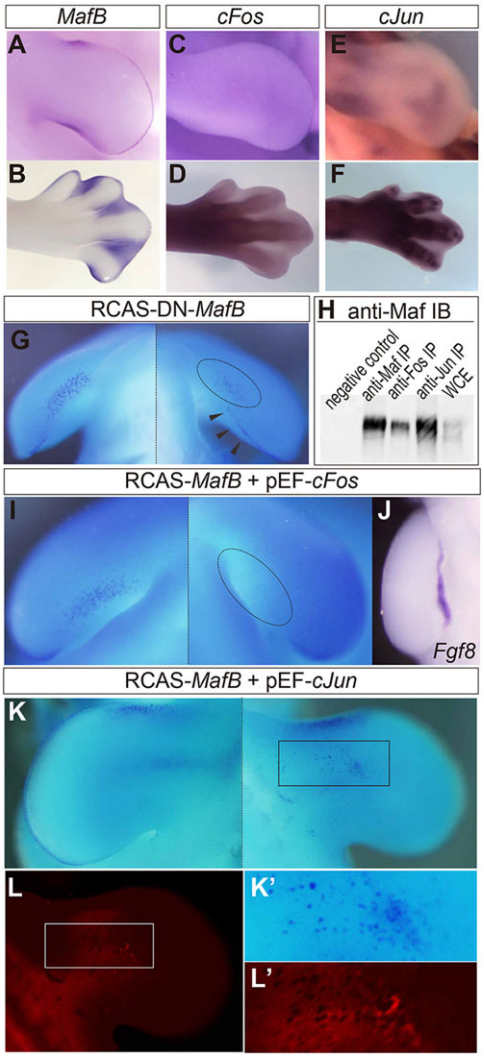

Fig. 1. MafB, cFos and cJun control the number of apoptotic cells in chick limb buds. (A-F) Expression of *MafB* (A,B), *cFos* (C,D) and *cJun* (E,F) in chick wing buds at stage 26 (A,C,E) and in chick leg buds at stage 31 (B,D,F). (G,I,K,L) Experimental (right) and control (left) wing buds of the same embryo were stained with Nile Blue 48 h after electroporation with RCAS-DN-*MafB* (G), a cocktail of RCAS-*MafB* and pEF-*cFos* (I), or a cocktail of RCAS-*MafB* and pEF-*cJun* (K,L). All constructs were electroporated together with either pCAGGS-*EGFP* or -*RFP*. Apoptosis was inhibited in the PNZ (dashed circle in G) but increased in the apical ridge (arrowheads in G) of wing buds that were electroporated with RCAS-DN-*MafB*. Apoptosis was inhibited in the PNZ of wing buds electroporated with a cocktail of RCAS-*MafB* and pEF-*cFos* (dashed circle in I), whereas it was increased in the area electroporated with a cocktail of RCAS-*MafB* and pEF-*cJun* (rectangles in K,L). (K′,L′) Higher-magnification images from K and L, respectively, as indicated. (H) Co-immunoprecipitation of endogenous Maf with Fos and Jun. Endogenous Maf, Fos and Jun were immunoprecipitated (IP) from lysates of stage 30 chick leg buds with anti-Maf, anti-Fos and anti-Jun antibodies, respectively. Immunoprecipitation with nonspecific IgGs was carried out as a negative control. Whole-cell extracts (WCE) and immunoprecipitation with anti-Maf antibody was carried out as a positive control. Co-immunoprecipitated MafB was detected by immunoblotting using anti-Maf. (J) *Fgf8* expression of experimental wing buds of embryos 48 h after electroporation with a cocktail of RCAS-*MafB* and pEF-*cFos*. The apical ridge formation was disrupted.

MafB/cFos inhibits apoptosis, whereas MafB/cJun promotes apoptosis

To investigate whether MafB has important roles in regulating apoptosis in chick limb buds, we introduced a retrovirus expressing the dominant-negative form of chicken MafB (DN-*MafB*), which lacks a transcriptional activation domain. Nile Blue staining of wing buds electroporated with the RCAS-DN-*MafB* construct showed that the number of apoptotic cells was reduced in the PNZ (5/6; dashed circle in Fig. 1G) and increased in the apical ridge (4/6; arrowheads in Fig. 1G), although control wing buds electroporated with a RCAS-*AP* vector did not display any changes in apoptosis (4/4; supplementary material Fig. S2A,B) or in the apical ridge formation (4/4; supplementary material Fig. S2C). These results suggest that AP-1 factor(s) that were inhibited by the RCAS-DN-*MafB* construct were involved in regulating the number of apoptotic cells in the apoptotic regions both in the mesenchyme and in the apical ectodermal ridge. By contrast, wing buds electroporated with RCAS-*MafB* showed almost no changes in apoptosis (6/7; supplementary material Fig. S2D,E), although they did form a considerably disturbed ridge (2/5; supplementary material Fig. S2F). Therefore, the phenotypes of wing buds electroporated with the RCAS-DN-*MafB* construct may be caused by suppression of multiple AP-1 factors, probably MafB and its heterodimer partner(s). We thus evaluated dimeric formation between endogenous MafB and cFos or cJun proteins using co-immunoprecipitation from lysates of stage 30 interdigital regions of distal leg buds. Maf did indeed interact with Fos and Jun in chick leg buds (Fig. 1H). We also examined whether MafB and cFos or cJun colocalized in chick limb buds by using antibodies against MafB, Fos, and Jun (supplementary material Fig. S3). Fos colocalized with MafB in interdigital regions of stage 30 chick leg buds (white arrowheads in supplementary material Fig. S3B). Likewise, Jun and MafB co-localized in interdigital regions at stage 30 (white arrowheads in supplementary material Fig. S3C). These results suggest that MafB proteins colocalize and interact with Fos and Jun proteins in interdigital regions of chick leg buds.

To investigate our hypothesis that MafB/cFos and MafB/cJun heterodimers are involved in regulating apoptosis in limb buds, we overexpressed *MafB* and either *cFos* or *cJun* constructs in limb buds. Electroporation of retrovirus constructs expressing *MafB* together with a human *cFos*-expressing pEF vector (Kataoka et al., 1994a) in the presumptive wing field led to the reduction of apoptotic cells in transfected areas, including the apical ridge (5/5; dashed circle in Fig. 1I), which caused the disruption of the apical ridge formation (5/7; Fig. 1J). By contrast, electroporation of RCAS-*MafB*, together with a human *cJun*-expressing pEF vector (Kataoka et al., 1994a) in the wing field caused ectopic apoptosis in the transfected regions (4/5; Fig. 1K-L′). These results suggest that, it in chick limb buds, MafB/cFos heterodimers repress apoptosis and MafB/cJun heterodimers promote it.

To confirm our hypothesis, we electroporated a Tol2-flanked construct expressing either *MafB* and *cFos* or *MafB* and *cJun* under

Development (2014) 141, 2885-2894 doi:10.1242/dev.099150

the control of a bipolar CMV promoter (pT2AL-*MafB*-BI-CMV-*cFos* in Fig. 2A; pT2AL-*MafB*-BI-CMV-*cJun* in Fig. 2B) along with a Tol2 transposase-expressing vector (pCAGGS-T2TP) (Kawakami and Noda, 2004) and pCAGGS-*EGFP* in the presumptive wing field at stage 14. Apoptotic cells in wing buds were examined with LysoTracker 2 days after electroporation. In mesenchymal cells of the PNZ (dashed circle in Fig. 2C′) and in ectodermal cells of the apical ridge (dashed circle in Fig. 2E) that were electroporated with pT2AL-*MafB*-BI-CMV-*cFos*, apoptosis was clearly repressed (10/13; Fig. 2C-F). Apoptosis was, however, ectopically activated both in mesenchymal and ectodermal cells (arrowheads in Fig. 2G′) of wing buds that were electroporated with pT2AL-*MafB*-BI-CMV-*cJun* (11/17; Fig. 2G,H). Thus, the co-existence of MafB and cFos repressed apoptosis, whereas co-existence of MafB and cJun promoted apoptosis both in mesenchymal and ectodermal cells of chick limb buds.

Overexpression and downregulation of *cFos* and *cJun* in chick wing buds

We electroporated pEF-*cFos* or -*cJun* alone into the PNZ of presumptive wing fields in stage 14-16 chick embryos and observed the effect on apoptosis after 48 h. Interestingly, overexpression of pEF-*cFos* alone in the PNZ caused both mild increases and decreases in the number of apoptotic cells (n=5; supplementary material Fig. S2G,H) and did not lead to any obvious changes in the apical ridge formation (5/5; supplementary material Fig. S2I). Electroporation of pEF-*cJun* alone produced only a slight increase in the number of apoptotic cells in some cases (5/7; supplementary material Fig. S2J,K) and did not lead to any alterations in the apical ridge formation (6/6; supplementary material Fig. S2L). Unlike MafB, both cFos and cJun have more than 10 other possible dimeric partners (Deppmann et al., 2006). Thus, electroporated cFos or cJun might have dimerized with other AP-1 transcription factors and may have activated both pro- and anti-apoptotic genes.

To investigate the function of endogenous *cFos* or *cJun*, we used siRNAs targeted to chick *cFos* or *cJun*. We first evaluated the effect of *cFos*-siRNA and *cJun*-siRNA *in vitro* by transfecting COS7 cells with *cFos*-siRNA and vectors expressing cFos-GFP fusion protein (pAc-*cFos-GFP*; supplementary material Fig. S4A) or with *cJun*-siRNA and vectors expressing cJun-GFP fusion protein (pAc-*cJun-GFP*; supplementary material Fig. S4B). At 24 h after transfection, the number of GFP-positive cells transfected with *cFos*-siRNA or *cJun*-siRNA was significantly reduced when compared with control cultures (P<0.00001, Student's t-test; supplementary material Fig. S4A,B). We then investigated the effect of depleting *cFos* or *cJun* in limb development 48 h after co-electroporation of *cFos*- or *cJun*-siRNA together with pCAGGS-*EGFP* into the PNZ of the presumptive wing region at stage 14-16 (supplementary material Fig. S4C-H). Interestingly, electroporation of *cFos*-siRNA led to both mild increases and decreases in the number of apoptotic cells (n=5; supplementary material Fig. S4E,F). By contrast, electroporation of *cJun*-siRNA in the wing field led to minimal changes in apoptosis (n=5; supplementary material Fig. S4G,H). It is possible that the freed partners of cFos or cJun dimerized with other AP-1 transcription factors after introduction of the *cFos*- or *cJun*-siRNA, and may have upregulated both pro- and anti-apoptotic genes. Control embryos in which control siRNA

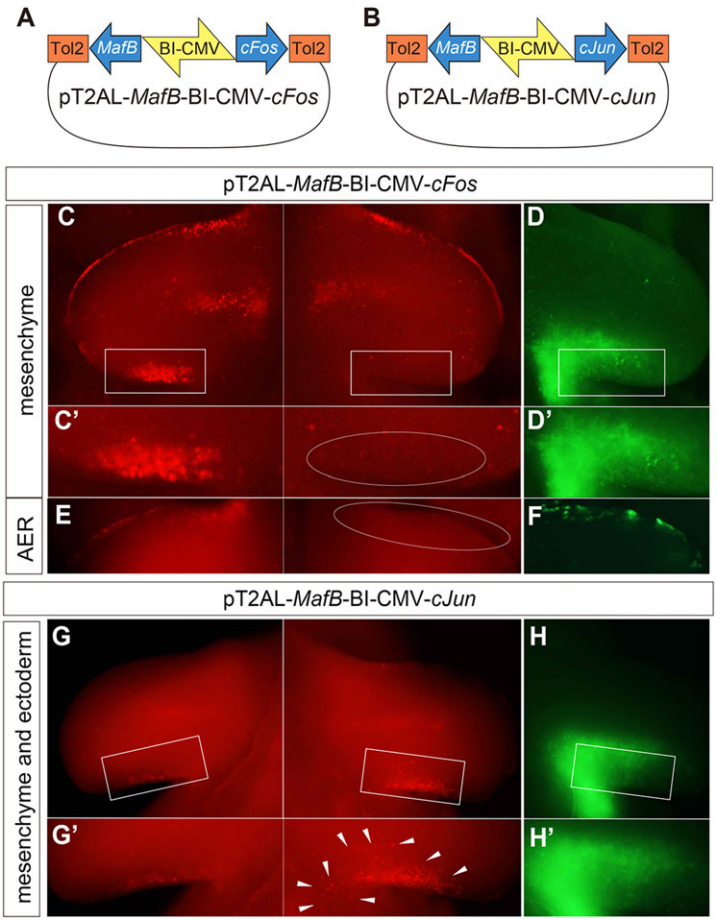

Fig. 2. Apoptosis is inhibited by MafB/cFos but is promoted by MafB/cJun in chick limb buds. (A,B) Diagrams of Tol2-flanked constructs pT2AL-*MafB*-BI-CMV-*cFos* (A) and pT2AL-*MafB*-BI-CMV-*cJun* (B). (C-H) Wing buds of stage 23 embryos electroporated with pT2AL-*MafB*-BI-CMV-*cFos* (C-F) or pT2AL-*MafB*-BI-CMV-*cJun* (G,H) were stained with LysoTracker (C,E,G), which labels apoptotic cells as well as healthy cells engulfing apoptotic debris. (C,E,G) Experimental (right) and control (left) wing buds of the same embryo. Constructs were electroporated together with pCAGGS-*EGFP* (D,F,H). (C′,D′,G′,H′) Higher-magnification images from C,D,G,H, respectively, as indicated. Cell death was repressed in the PNZ (dashed circle in C′) and the apical ectodermal ridge (dashed circle in E) of wing buds electroporated with pT2AL-*MafB*-BI-CMV-*cFos*. Cell death was increased in both the ectoderm and mesoderm of wing buds electroporated with pT2AL-*MafB*-BI-CMV-*cJun* (arrowheads in G′).

Development (2014) 141, 2885-2894 doi:10.1242/dev.099150

and pCAGGS-*EGFP* were electroporated did not show any changes in apoptosis (n=3; supplementary material Fig. S4C,D).

Function of other AP-1 transcription factors

As seen in supplementary material Fig. S1, genes encoding other AP-1 transcription factors were also expressed in the apoptotic regions (e.g. *c-maf*, *Nfe2l1*, *Nfe2l2*, *Xbp1*). We examined whether *c-maf*, *Nfe2l1*, *Nfe2l2* and *Xbp1* could affect the number of apoptotic cells by introducing vectors that express those genes into the PNZ of stage 14-16 chick wing buds (supplementary material Fig. S5). Misexpression of *c-maf, Nfe2l2* and *Xbp1* in wing buds showed hardly any changes in apoptosis (3/5, 5/6 and 4/5, respectively), whereas that of *Nfe2l1* showed only a mild reduction in apoptosis in some cases (4/6; dashed circle in supplementary material Fig. S5C). Thus, it is possible that AP-1 transcription factors other than MafB, cFos and cJun, including Nfe2l1 and its unknown dimeric partners, are also involved in regulating the number of apoptotic cells in chick limb buds.

Expression of MafB, but not cFos or cJun, is regulated by BMP signalling in limb buds

Apoptosis in limbs is controlled by BMP signalling (Ganan et al., 1996; Macias et al., 1997; Tang et al., 2000; Yokouchi et al., 1996; Zou and Niswander, 1996). We thus investigated whether expression of *MafB*, *cFos* and *cJun* was regulated by BMP signalling. For this purpose, we inserted a bead soaked with BMP2, Noggin or PBS into stage 28 leg buds. Twenty-four hours after implantation, expression of *MafB* was activated by BMP2 (5/8; arrowheads in Fig. 3A) and repressed by Noggin (6/7; dashed circle in Fig. 3B), suggesting that *MafB* expression in the INZ is controlled by BMP signalling. By contrast, expression of *cFos* and *cJun* showed no changes after implantation of a bead soaked with BMP2 (5/5, Fig. 3C; 5/5, Fig. 3E) or Noggin (5/5, Fig. 3D; 4/4, Fig. 3F). No changes were observed in the expression of *MafB*, *cFos* or *cJun* after implantation of a PBS-soaked bead (4/4, 5/5 and 5/5, respectively; supplementary material Fig. S6A-C). These results suggest that expression of *MafB*, but not *cFos* or *cJun*, is controlled by BMP signalling. Similarly, ectopic *MafB* expression was induced in the PNZ of stage 24 wing buds 24 h after implantation of a BMP-soaked bead (7/7; Fig. 3G). By contrast, no changes were seen in *MafB* expression after application of a PBS-soaked bead (4/4; supplementary material Fig. S6D). We then investigated expression of *MafB* 3 h after implantation of a BMP2-soaked bead in the INZ at stage 28. As seen in Fig. 3H, ectopic *MafB* expression was induced around a BMP2-soaked bead (6/6; Fig. 3H), but not around a PBS-soaked bead (5/5; supplementary material Fig. S6E). Therefore, *MafB* is most likely directly regulated by Smads, phosphorylated by serine/threonine kinases BMP receptors, or through only a few intermediate transcription factor(s), in this signalling pathway.

Retinoic acid signalling is specifically active in the interdigital region (Lussier et al., 1993; Rodriguez-Leon et al., 1999) and is sufficient to trigger interdigital apoptosis (Alles and Sulik, 1989; Dupe et al., 1999; Hernandez-Martinez et al., 2009). To see whether *MafB* expression is controlled by retinoic acid signalling in chick limb buds, we implanted a retinoic acid-soaked bead into the PNZ of stage 21-22 wing buds and into the INZ of stage 28 leg buds and examined expression of *MafB* (Fig. 3I,J). Twenty-four hours after application of a retinoic acid-soaked bead, expression of *MafB* was weakly activated around the bead in the PNZ (3/4; arrowheads in Fig. 3I) and slightly activated in a single case in the INZ (1/9; arrowheads in Fig. 3J). By contrast, no obvious changes were observed after implantation of a DMSO-soaked bead in the PNZ and in the INZ (5/5 and 6/6, respectively; supplementary material Fig. S6F,G). Thus, expression of *MafB* seems to be only weakly activated by retinoic acid in early limb buds.

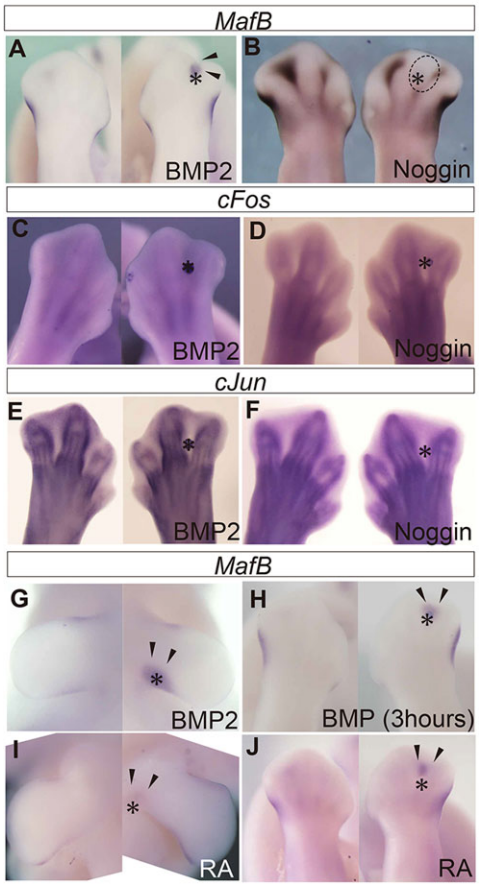

Fig. 3. Expression of *MafB* is regulated by BMP signalling and retinoic acid signalling in limb buds. (A-J) Expression of *MafB* (A,B,G-J), *cFos* (C,D) and *cJun* (E,F). (A-F) Twenty-four hours after implantation of a bead (asterisk) soaked with BMP2 (A,C,E) or Noggin (B,D,F) in the INZ of right leg buds at stage 28, *MafB* expression was increased near the BMP2-soaked bead (arrowheads in A) and decreased near the Noggin-soaked bead (dashed circle in B). No detectable changes in *cFos* or *cJun* expression were observed (C-F). (G) Twenty-four hours after implantation of a bead (asterisk) soaked with BMP2 in the PNZ of the right wing bud at stage 21-22. *MafB* expression was increased near the BMP2-soaked bead (arrowheads). (H) Three hours after implantation of a BMP2-soaked bead (asterisk) in the INZ of the right leg bud at stage 28. Ectopic expression of *MafB* was observed around the BMP2-soaked bead (arrowheads). (I,J) Twenty-four hours after implantation of a retinoic acid (RA)-soaked bead in the PNZ of the right wing bud at stage 21-22 (I), or in the INZ of the right leg bud at stage 28 (J). Right (experimental) and left (control) limb buds of the same embryo are shown.

Maf proteins are detected both in macrophage-positive and -negative regions in limb buds

In the hematopoietic system, *MafB* is expressed at high levels in macrophages and promotes macrophage differentiation (Bakri et al., 2005; Kelly et al., 2000). To investigate whether *MafB* expression in the limb buds is due to the presence of macrophages, we examined the distribution of macrophages and MafB proteins in interdigital regions of stage 30 leg buds (supplementary material Fig. S3D,E). Double staining of leg buds with macrophage and MafB antibodies showed that MafB proteins were distributed in macrophages (white arrowheads in supplementary material Fig. S3D). MafB proteins were also distributed in nuclei of several non-macrophage cells in

Development (2014) 141, 2885-2894 doi:10.1242/dev.099150

interdigital regions (open arrowheads in supplementary material Fig. S3E).

Identification of Maf and Jun binding sites

We then decided to look for downstream targets of MafB/cJun heterodimers that promote apoptosis in chick limb buds. To identify target genes and regulatory elements controlled by Maf and Jun, we dissected the distal region of 60 leg buds from stage 30 chick embryos (Fig. 4A) and performed ChIP using these tissue samples with Maf, Jun or p300 antibodies (Fig. 4C-E). Epigenomic profiling of p300, a transactivational co-activator, identifies active enhancers (Visel et al., 2009). Immunoprecipitated DNA fragments were analysed using massively parallel sequencing, and the resulting 50 base pair (bp) sequence reads were aligned with the reference chick genome (galGal3).

In leg buds, we identified 26,009, 29,815 and 18,303 regions of the genome with substantial enrichment in sequences associated with Maf, Jun and p300, respectively (in all cases, the presence of binding sites was indicated by fold enrichment >2.5 and peak width >400 bp; supplementary material Table S2). To identify direct targets of MafB/cJun heterodimers in chick limb buds, we looked for Maf and Jun binding sites that were coincident with p300 binding sites and identified 1347 peaks (supplementary material Table S3). Of these, the transcriptional start sites (TSSs) of 1717 genes resided within ±50 kb of these identified peaks, and these genes were highly expressed in limb buds based on published transcriptome data (normalized counts ≥100; supplementary material Table S4) (Wang et al., 2011). We considered genes that were within ±50 kb of these identified peaks as potential target genes of MafB/cJun heterodimers in chick limb buds. To select candidates among potential target genes of AP-1 (supplementary material Table S4), we looked for genes encoding core components that regulate the cell cycle and/or apoptosis (supplementary material Table S5); we identified *p73*, *Chk1* and *DAPK1* (Fig. 4D; supplementary material Fig. S7). An AP-1 binding site was also found near the TSS of caspase 6, but we did not choose caspase 6 as a candidate because *Casp6* knockout mice exhibit normal limb phenotype (Zheng et al., 1999). In addition, we selected *p63* as a potential AP-1 target, as *p63* belongs to the same family as *p73* (Fig. 4C). Furthermore, a possible binding site for AP-1 proteins that was coincident with a p300 binding site was identified within ±50 kb of TSSs of *p63*, and transcription of *p63* is controlled by AP-1 transcription factors (Leventaki et al., 2007; Vartanian et al., 2011; Yao et al., 2010). To see whether these candidates are expressed in the apoptotic regions, we examined their expression patterns in stage 26 chick wing buds and stage 31 chick leg buds (Fig. 4F-K; supplementary material Fig. S7). Of these, *p63*, *p73* and *Chk1*, but not *DAPK1*, were highly expressed in chick limb buds, including apoptotic regions (Fig. 4F-K) such as the apical ridge (*p63* in Fig. 4F) and the mesenchyme (*p73* and *Chk1* in Fig. 4H-K). Chk1 initiates cell cycle arrest when ATM and/or ATR recognizes DNA damage, and they induce transcription of *p73*, which mediates apoptosis (Fig. 4B; Urist et al., 2004). p63 can also induce apoptosis (Fig. 4B; Pyati et al., 2011).

To investigate whether MafB/cJun control the transcription of candidate target genes during limb development, we misexpressed RCAS-*MafB* together with pEF-*cJun* in the presumptive wing field at stage 14 and examined the expression patterns of potential target genes (Fig. 5A,B; supplementary material Fig. S8A). Thirty-six hours after misexpression, *p63* and *p73*, but not *Chk1*, were ectopically expressed in the region electroporated with RCAS-*MafB*, pEF-*cJun* and pCAGGS-*RFP* (*p63*, 6/6, arrowheads in Fig. 5A; *p73*, 5/7, arrowheads in Fig. 5B; *Chk1*, 0/6, see supplementary material Fig. S8A). Expression of *p63* and *p73* was not altered after misexpression of control constructs (5/8 and 2/3, respectively; supplementary material Fig. S8B,C). These results suggest that expression of *p63* and *p73* is controlled by MafB/cJun.

Binding profiles suggest that AP-1 binds within the first intron of *p63* (BS-*p63*; Fig. 4C) and 8.5 kb upstream of *p73* (BS-*p73*; Fig. 4D). To confirm binding of p300 in these regions, we carried out ChIP-qPCR analysis with stage 30 chick leg buds using anti-p300 (supplementary material Fig. S9). ChIP-qPCR analyses showed distinct degrees of enrichment of p300 binding to BS-*p63* and BS-*p73* (supplementary material Fig. S9). These results suggest that p300 binds to these AP-1 binding sites.

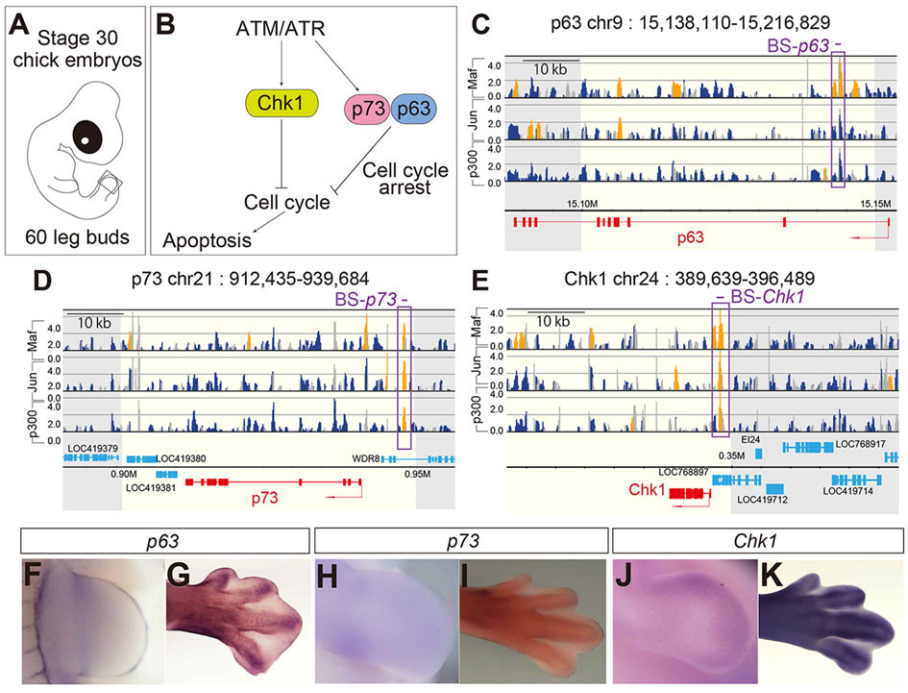

Fig. 4. Binding regions for Maf and Jun identified by using ChIP-seq assay. (A) Sixty hindlimb autopods were dissected from stage 30 chick embryos. (B) Core regulators required for the checkpoint machinery of the cell cycle. (C-E) Binding regions and associated genes were revealed by ChIP-seq assay using chick embryo tissue samples with Maf, Jun or p300 antibodies. DNA fragments tested in reporter assays are shown in each panel [*p63* (C), *p73* (D) and *Chk1* (E)] as purple boxes. Coordinates (galGal3) are shown above each graph, and the NCBI RefSeq transcripts are shown below. Yellow lines indicate regions with more than 2.5-fold enrichment (peak width >400 bp). (F-K) Expression patterns of *p63* (F,G), *p73* (H,I) and *Chk1* (J,K) in wing buds at stage 26 (F,H,J) and in leg buds at stage 31 (G,I,K).

Development (2014) 141, 2885-2894 doi:10.1242/dev.099150

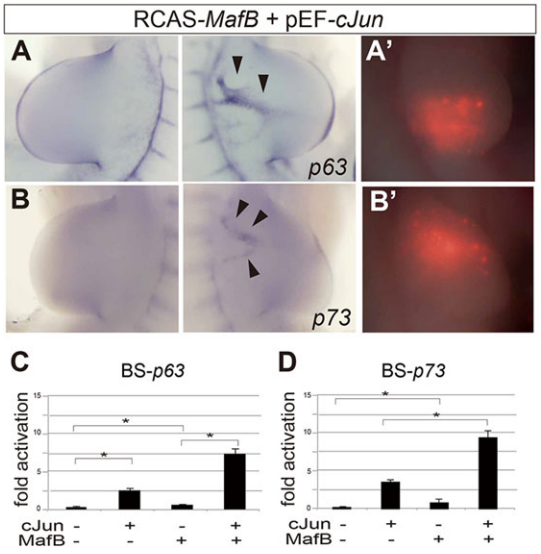

Fig. 5. MafB/cJun activate expression of *p63* and *p73* in chick limb buds. (A,B) Expression of *p63* (A) and *p73* (B) in chick wing buds 36 h after electroporation with a cocktail of RCAS-*MafB*, pEF-*cJun* and pCAGGS-*RFP*. Right (experimental) and left (control) wing buds of the same embryo are shown. (A′,B′) The electroporated sites were visualized with RFP. Arrowheads indicate activated expression of *p63* (A) and *p73* (B). (C,D) The binding sites were tested in reporter assays. Data are mean±s.d., **P*<0.05 (Student's *t*-test).

To test the functions of these AP-1-binding sites, each identified site was cloned directly in front of a minimal promoter that is followed by a luciferase reporter to test whether it is responsive to MafB/cJun transactivation (Fig. 5C,D). Transient reporter assays showed that the enhancer activities of BS-*p63* and BS-*p73* were highly activated by co-expression of cJun and MafB (Fig. 5C,D), suggesting that BS-*p63* and BS-*p73* can function as enhancer elements to control gene expression in limb buds, and that their activities are dependent on MafB and cJun. These results suggest that MafB/cJun heterodimers directly activate *p63* and *p73* and promote apoptosis. Taken together, our data demonstrate that dimeric combinations of MafB, cFos and cJun control the apoptosis-survival balance and that MafB/cJun heterodimers trigger apoptosis by activating expression of *p63* and *p73* during chick limb morphogenesis (Fig. 6).

DISCUSSION

We showed that MafB/cJun promotes apoptosis both in mesenchymal cells and in the apical ectodermal ridge, although it is likely that this heterodimer acts through different targets in the two regions. For example, one target, *p63*, is expressed only in the ectoderm. A p63/p73-responsive element is present in the second intron of *Jagged1* (Sasaki et al., 2002), which is one of a few components known to control apoptosis in the apical ridge (Francis et al., 2005). Furthermore, p63 and p73 are required for triggering p53-dependent apoptosis in response to DNA damage (Flores et al., 2002). By contrast, p63 also directly upregulates the expression of *Dlx5* (Kouwenhoven et al., 2010), which promotes proliferation in the median apical ridge (Robledo et al., 2002), and *p63* knockout mice fail to form the apical ectodermal ridge (Mills et al., 1999; Yang et al., 1999). p63 in the apical ectodermal ridge likely activates multiple genes, as it is known to do in other systems (Melino et al., 2003). Such genes may be involved in pro-apoptotic cascades (including *Jagged1*) and proliferation (including *Dlx5*), and the sum of all signals is likely to determine the fate of cells. Further studies are required to determine the detailed functions of p63 targets that regulate the formation of the apical ridge. p73 contributes to p53-independent apoptosis by directly activating expression of *PUMA*, *Bax* and *p21* (Urist et al., 2004). p73 also activates transcription of *Noxa*, mutation of which causes mitochondrial dysfunction (Flinterman et al., 2005). In agreement with these p73 functions, *Bax* is specifically expressed in the INZ (Dupe et al., 1999), and mice deficient in both *Bax* and *Bak* show soft-tissue syndactyly (Lindsten and Thompson, 2006). Thus, in apoptotic regions of chick limb buds, p73 very likely triggers a p53-independent apoptosis cascade probably by activating *Bax*. However, in mice, the absence of *p73* does not affect limb development (Yang et al., 2000). This may be because levels of *p73* transcripts are very low in mouse limb buds (EMBRYS; http://embrys.jp/embrys/html/MainMenu.html; Yokoyama et al., 2009) when compared with those in chick limb buds (Fig. 4H,I). In this study, we looked for only direct targets of MafB/cJun, the functions of which could explain the phenotypes noted here; it is also reasonable to expect that MafB/cFos directly activate pro-apoptotic genes. Importantly, several other AP-1 family members activate both pro-apoptotic and anti-apoptotic genes (Shaulian and Karin, 2002). Indeed, Shaulian and Karin (2002) proposed that there is a 'balance between the pro-apoptotic and anti-apoptotic target-genes that determines whether the final outcome will be cell survival or cell death'. Hence, we must consider the possibility that MafB/cFos and Maf/cJun activate both pro- and anti-apoptotic genes, and that the balance between these activated genes determines the outcome. Furthermore, MafB/cFos and/or MafB/cJun are likely also to inhibit the expression of pro-apoptotic or survival genes, and cFos/cJun combinations may also control the expression of genes throughout limb buds. For example, MafB/cJun binds to the regulatory region of *Hoxb9* to repress its transcription (Mechta-Grigoriou et al., 2003), and cFos/cJun stably binds to regulatory elements in many other systems (Shaulian and Karin, 2002). Although MafB seems to dimerize with either cFos or cJun in chick limb buds (Fig. 1H; supplementary material Fig. S3B,C), both cFos and cJun have more than 10 other possible dimer partners (Deppmann et al., 2006). As we have shown in supplementary material Figs S2 and S4, overexpression or knockdown of *cJun* alone produced only a slight increase or decrease in the number of apoptotic cells in some cases. Moreover, overexpression or knockdown of *cFos* alone both increased and decreased the number of apoptotic cells (supplementary material Fig. S2G,H and Fig. S4E, F). These results suggest that cFos and cJun can dimerize with other AP-1 transcription factors and activate both pro- and anti-apoptotic genes. It is also plausible that other combinations of AP-1 transcription factors have roles that are similar to those of MafB, cFos and cJun in regulating apoptosis during limb morphogenesis.

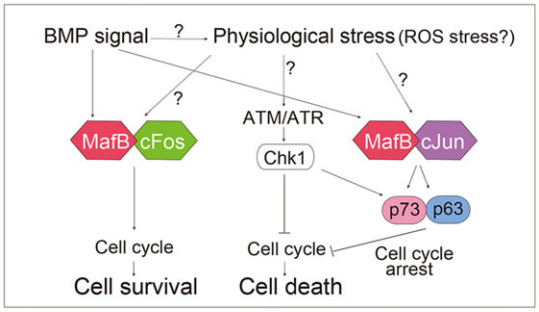

Fig. 6. Mechanisms that control the apoptosis-survival balance during chick limb development. Dimeric combinations of MafB, cFos and cJun control the apoptosis-survival balance in limb patterning.

Development (2014) 141, 2885-2894 doi:10.1242/dev.099150

In fact, misexpression of *Nfe2l1* caused mild repression of apoptosis in chick limb buds (supplementary material Fig. S5). Although overexpression of *c-maf*, *Nfe2l2* or *Xbp1* resulted in minimal changes in the number of apoptotic cells (supplementary material Fig. S5), it is still possible that they are also involved in this process by forming heterodimers or are involved in the development of different structures in the embryo. Future studies should clarify the complex regulation of AP-1 factors in various morphological processes.

In this study, we show that MafB is involved in controlling apoptosis in chick limb buds. Importantly, a recent study in mice revealed a novel function for MafB in inhibiting foam-cell apoptosis, which in turn accelerates atherogenesis (Hamada et al., 2014). By contrast, *MafB*-deficient mice have phenotypically normal limbs (Satoru Takahashi, personal communication). Notably, however, the expression of many AP-1 family members, including *MafB* and *cFos*, differs between the limb buds of chick and mouse embryos (supplementary material Fig. S1; EMBRYS; Yokoyama et al., 2009). In mice, *MafB* is not expressed in the apical ridge and *cFos* transcripts are not detectable in limb buds (EMBRYS; Yokoyama et al., 2009). Furthermore, mouse limb buds show very few anterior and posterior mesenchymal regions that undergo apoptosis comparable with that observed in the chick. Such differences may explain why *MafB* mutant mice show relatively normal limb phenotypes. It is therefore likely that other AP-1 transcription factors in mouse limb buds play roles similar to those of MafB and cFos in chick limb buds.

The dimerization of Maf with Fos or Jun probably depends on the amount of each of these proteins in a cell and their relative binding affinities. Protein dimerization rates depend on the amounts of the respective molecules and on the Arrhenius activation energies for their dimerization (Ecevit et al., 2010). In fact, dose-dependent heterodimer formation of Maf with Fos and Jun has been demonstrated with a protein dimerization assay (Kataoka et al., 1994b).

AP-1 transcription factors control gene expression induced by free radicals (Sen and Packer, 1996). Interestingly, high levels of ROS have been detected in the INZ of limb buds, and the number of apoptotic cells was reduced after treatment with antioxidants in limb buds (Salas-Vidal et al., 1998; Schnabel et al., 2006). Moreover, both cFos and cJun are regulated by oxidants at both the transcriptional and translational levels (Sen and Packer, 1996). It is thus fascinating to speculate that transcription of MafB is induced by ROS stress in chick limb apoptotic regions; future studies will be required to link ROS stress and MafB functions during apoptosis. In this study, we show that expression of MafB is regulated by BMP signalling in limb buds. As MafB is able to either activate or inhibit apoptosis depending on its heterodimer partner (i.e. cJun or cFos, respectively), BMP probably also activates other factors that trigger apoptosis in limbs. During osteoblast differentiation, BMP induces a Nox4-derived ROS production (Mandal et al., 2011). Levels of ROS and/or antioxidant enzymes may also be regulated by BMP in limb buds as suggested previously (Schnabel et al., 2006). We have thus developed a model in which AP-1 factors are involved in controlling apoptosis in developing limb buds (Fig. 6). MafB/cFos heterodimers reduced the numbers of dying cells in apoptotic regions of chick limb buds. MafB/cJun heterodimers trigger apoptosis in chick limb buds, and they directly activate expression of *p63* and *p73*, key factors known to arrest the cell cycle, leading to the activation of apoptosis.

BMP signalling activates expression of *MafB* and possibly upregulates the level of ROS in apoptotic regions (Schnabel et al., 2006). ROS stress itself may activate the expression of the AP-1 factors MafB, cFos and/or cJun in limb buds, as shown in other systems (Sen and Packer, 1996). We conclude that the balance of MafB and cFos or cJun heterodimer combinations, specifically in apoptotic regions, controls the apoptosis-survival balance, and MafB/cJun heterodimers trigger apoptosis by activating expression of *p63* and *p73* during limb patterning in chick embryos.

MATERIALS AND METHODS

Whole-mount *in situ* hybridization

The *A9300001N09Rik*, *Atf1*, *Atf2*, *Atf3*, *Atf4*, *Atf6*, *Bach1*, *Bach2*, *Batf*, *Batf3*, *CEBPd*, *CEBPg*, *Creb1*, *Creb3*, *Creb3l1*, *Creb3l2*, *Creb3l3*, *Creb5*, *Crebl2*, *Crem*, *cFos*, *HLF*, *cJun*, *Nfe2l1*, *Nfe2l2*, *Nfil3* and *Xbp1* probes were transcribed from Biotechnology and Biological Sciences Research Council (BBSRC; http://www.chick.manchester.ac.uk/) chick EST cDNA clones (ChEST595m10, ChEST547e5, ChEST913d17, ChEST927o11, ChEST390a19, ChEST222o13, ChEST926l10, ChEST1024h14, ChEST543k2, ChEST372f15, ChEST704p8, ChEST86h12, ChEST50d14, ChEST256g16, ChEST335l1, ChEST553f15, ChEST98d7, ChEST964l8, ChEST860a20, ChEST72i15, ChEST262m21, ChEST837k20, ChEST520g15, ChEST719p8, ChEST813j4, ChEST567h3 and ChEST151f18, respectively) (Boardman et al., 2002; Hubbard et al., 2005). *Atf7*, *CEBPa*, *CEBPb*, *Fosl2* and *Jund* probes were transcribed from the University of Delaware Chick EST cDNA clones (pgf1n.pk008.b16, pgl1n.pk007.g3, pgm2n.pk007.i18, pgn1c.pk014.g7 and pgl1n.pk012.d17, respectively; http://www.chickest.udel.edu/). *Crebzf*, *JDP*, *MafF*, *MafG*, *MafK*, *TEF*, *p63*, *p73*, *Chk1* and *DAPK1* cDNAs for *in situ* probes were amplified from cDNA pools prepared from stage 20-28 chick embryos using primers that hybridize to the published sequences described in supplementary material Table S1. The *L-Maf*, *MafB*, *c-maf* and *Fgf8* probes were transcribed as described previously (Crossley et al., 1996; Kataoka et al., 1994a). Whole-mount *in situ* hybridization was performed as described previously (Wilkinson, 1992).

Plasmid construction

For RCAS-*MafB*, the open reading frame (ORF) of chick *MafB* was amplified using primers that include the *Eco*RI, Kozak and FLAG epitope sequences at the N terminus and the *Hin*dIII sequence at the C terminus (5′-CCGGAATTCCCCACCATGGACTACAAGGACGATGACGATAAGATCGGCTCCCACCAAGTGTC-3′ and 5′-CCCAAGCTTGCACTCACATGAAGAACTCG-3′; all PCR primers given as forward and then reverse). The resulting PCR products were inserted into the pGEM-T Easy vector (Promega; pGEMTeasy-*MafB*) and then cloned into the *Eco*RI and *Hin*dIII sites of SLAX12 NCO (Morgan and Fekete, 1996). A *Cla*l fragment was cloned into the *Cla*l site of the RCAS-*AP* retroviral vector (Homburger and Fekete, 1996; Hughes et al., 1987). For DN-*MafB*, the cDNA sequence encoding amino acid residues 111 to 311 of chick *MafB* was amplified with PCR using primers including the *Eco*RI, Kozak and FLAG epitope sequences at the N terminus and the *Hin*dIII sequence at the C terminus (5′-CCGGAATTCCCCACCATGGACTACAAGGACGATGACGATAAGGGTGGTATGGCCGGAGAGCTGAGCATC-3′ and 5′-CCCAAGCTTGCACTCACATGAAGAACTCG-3′), inserted into the pGEM-T Easy vector and then cloned into SLAX12 NCO. A *Cla*l fragment was cloned into the *Cla*l site of the RCAS-*AP* retroviral vector. For pEF-*MafB*, the ORF of chick *MafB* was amplified using specific primers (5′-ATCCTCTAGAGTCGACCCACCATGGACTACAAGGA-3′ and 5′-TAAAGGGAAGCGGCCGCACTCACATGAAGAACTCG-3′) and cloned into the *Not*I and *Sal*I sites of the pHyg-EF2 vector (Nishizawa et al., 2003) via the In-Fusion reaction (Clontech). For pT2AL-*MafB*-BI-CMV-*cFos* and pT2AL-*MafB*-BI-CMV-*cJun*, pBI-CMV1 (Clontech) was digested with *Sac*I and *Sal*I (for pBSK-CMV1) or with *Xho*I and *Xba*I (for pBSK-CMV2) and subcloned into the pBSK^{-} vector (pBSK-CMV1 and pBSK-CMV2, respectively). Then, a polyA tail sequence was amplified with specific primers (for pBSK-CMV1, 5′-TAAAGCGGCCGCCACCGCGG-3′ and 5′-ACGCGTCGACTAGATCTGATCTAGAGGATC-3′; for pBSK-CMV2, 5′-CGCGGATCCAAGCTTGATGATCCAGACATGATAAG-3′ and 5′-GGACTAGTCTCGAGGATCTAGAGGATCATAATCA-3′) using pT2AL200R150G (Urasaki et al., 2006) as a template and cloned into the *Not*I and *Sal*I sites of pBSK-CMV1 (pBSK-CMV1-pA) and the *Bam*HI and *Spe*I sites of pBSK-CMV2, to incorporate the polyA tail sequence at the C terminus (pBSK-CMV2-pA).

Development (2014) 141, 2885-2894 doi:10.1242/dev.099150

Then, SLAX12 Nco-*cFos* and SLAX12 NCO-*cJun* were digested with *Hin*dIII and *Cla*I, and the ORFs of human *cFos* and *cJun* were cloned into the pBSK$^-$ vector. The ORFs of human *cFos* and *cJun* were then subcloned into the *Not*I and *Cla*I sites of pBSK-CMV1-pA (pBSK-CMV1-*cFos*-pA and pBSK-CMV2-*cJun*-pA, respectively). Then, the ORF of chick *MafB* from pGEMTeasy-*MafB* was digested with *Eco*RI and *Hin*dIII and cloned into the *Eco*RI and *Hin*dIII sites of pBSK-CMV2-pA (pBSK-CMV2-*MafB*-pA). pBSK-CMV1-*cFos*-pA and pBSK-CMV2-*cJun*-pA were digested with *Xho*I and *Bgl*II, and cloned into pT2AL200R150G. pBSK-CMV2-*MafB* was digested with *Xho*I, and the DNA fragment was cloned into the *Xho*I site of pT2AL200R150G-CMV1-*cFos*-pA and pT2AL200R150G-CMV2-*cJun*-pA (pT2AL-*MafB*-BI-CMV-*cFos* and pT2AL-*MafB*-BI-CMV-*cJun*, respectively) using the In-Fusion reaction. The genomic regions of the AP-1-binding site peaks were amplified with PCR using primers described in supplementary material Table S1 and were cloned into a minimum promoter containing the pGL4.23 [*luc2*/miniP] vector (Promega).

In ovo DNA electroporation

The plasmid solutions or small interfering RNAs (siRNAs; see below) were coloured with 2.5-5% Fast Green and co-electroporated with pCAGGS-*EGFP* (a gift from Dr J. Miyazaki and Dr T. Ogura) (Niwa et al., 1991) or pCAGGS-*RFP* (Das et al., 2006) into the presumptive limb mesenchyme as described previously (Ogura, 2002). Briefly, the solution was injected into the lateral plate mesoderm of stage 14-16 chick embryos, and two pulses of 8-12 V and 80-90 ms were applied. The concentrations of the prepared plasmid solutions and siRNAs were as follows: RCAS-*MafB*, 6.2 mg/ml; pEF-*cFos*, 6.6 mg/ml; pEF-*cJun*, 6.4 mg/ml; pCAGGS-*EGFP*, 3.5 mg/ml; pCAGGS-*RFP*, 6.0 mg/ml; pT2AL-*MafB*-BI-CMV-*cFos*, 5.2 mg/ml; pT2AL-*MafB*-BI-CMV-*cJun*, 6.9 mg/ml; pCAGGS-T2TP, 8.0 mg/ml; RCAS-*AP*, 5.5 mg/ml; pHygEF2, 4.7 mg/ml; pEF-*c-maf*, 9.8 mg/ml; pMSCV-*Nfe2l1*, 7.0 mg/ml; pcDNA3-*Nfe2l2*, 8.1 mg/ml; pCMV-*Xbp1*, 6.4 mg/ml; control siRNA, 250 µM; *cFos* siRNA, 250 µM; and *cJun* siRNA, 250 µM.

Morphological analysis of the limb

The morphology of the limbs that were subjected to experimental manipulation was studied after cartilage staining with Alcian Blue. The pattern of apoptosis was analysed with vital staining with Nile Blue and LysoTracker Red (Invitrogen) (Mariani et al., 2008).

Co-immunoprecipitation

Co-immunoprecipitation (co-IP) was carried out as described previously (Chen et al., 2004). Briefly, interdigital regions of stage 30 limb buds were dissected from 10 embryos in PBS, and lysed in lysis buffer [10 mM HEPES (pH 7.5); 420 mM NaCl; 0.5% NP-40; 0.2% protease inhibitors (BioVision)] on ice for 25 min with trituration. Lysates were centrifuged at 2500 ***g*** for 5 min, and the supernatants were transferred into new tubes. The Maf antibody (Santa Cruz; sc-7866), the Fos antibody (Santa Cruz; sc-52), the Jun antibody (Santa Cruz; sc-1694) or the normal rabbit IgG (PeproTech EC) used for co-IP was covalently cross-linked to Dynabeads (Veritas), and bound proteins were detected on western blots with affinity-purified anti-Maf.

Insertion of beads into limb buds

CM Affi-Gel Blue Gel (Bio-Rad) beads were loaded with 0.1 mg/ml BMP2 (R&D Systems), 1 mg/ml Noggin (R&D Systems) or PBS (Tumpel et al., 2002). AG1-X2 resin beads (Bio-Rad) were loaded with 10 mg/ml all-*trans* retinoic acid (Sigma) or dimethyl sulfoxide (DMSO). Then a single bead was inserted into the PNZ of stage 21-22 chick wing buds or the interdigital area of stage 28 chick embryos. Embryos were fixed 24 h later in 4% paraformaldehyde and then subjected to *in situ* hybridization as described above.

Immunohistochemistry

Fluorescent immunostaining was performed on cryosections of limb buds at stage 30 as described previously (Bangs et al., 2011). Primary antibodies used were anti-MafB (Santa Cruz; sc-10022), anti-Fos, anti-Jun and anti-macrophage (Acris Antibodies; AM08143PU-N). Confocal images were taken on a LSM780 confocal microscope (Carl Zeiss).

siRNA preparation

siRNAs specific for chicken *cFos* and *cJun* and a control siRNA were obtained from Invitrogen (Stealth RNAi). The targeted sequence was 5′-TCAACGACTTCGACCTGATGAAGTT-3′ (coding region 127-151 of chick *cFos*; GenBank accession number NM_205508) and 5′-AGA-AGAGCCTCAGACTGTACCTGAA-3′ (coding region 615-639 of chick *cJun*; GenBank accession number NM_001031289).

Cell culture and transfection

COS7 cells were maintained in DMEM supplemented with 10% FBS, 100 U/ml penicillin and 100 µg/ml streptomycin. Co-transfection of target plasmids (pAc-*cFos-GFP* or pAc-*cJun-GFP*) and siRNAs was carried out with Lipofectamine 2000 (Invitrogen) following the manufacturer's protocol. To assess the efficiency of the siRNAs on pAc-*cFos-GFP* or pAc-*cJun-GFP* expression in COS7 cells, the number of GFP-positive cells was counted 24 h after transfection. Student's *t*-test was performed to assess the differences between numbers of cells transfected with siRNA ($P<0.00001$). For reporter assays, COS7 cells were plated on 24-well plates and transfected using Lipofectamine 2000 and a total of 2.4 µg of DNA. Reporter constructs were co-transfected with 0.8 µg of *MafB* and/or *cJun* expression constructs in combination with *Renilla* vectors. Cells were collected 24 h post-transfection, and luciferase reporter assays were performed using the Dual Luciferase Kit (Promega). Each assay was performed twice.

Chromatin immunoprecipitation sequencing (ChIP-Seq) and qPCR (ChIP-qPCR)

ChIP was performed using leg buds at stage 30. Sixty limb buds were dissected, fixed in 1% formaldehyde for 10 min at room temperature, washed with PBS, and stored at −80°C. ChIP was performed from these tissue samples using antibodies against Maf, Jun or p300 (Santa Cruz; sc-584) as described previously (Visel et al., 2009). DNA samples from the whole-cell extract (WCE) and ChIP fractions were further sheared with an ultra sonicator, ligated to sequencing adapters and amplified according to the manufacturer's instructions. Gel-purified amplified DNA (100-150 bp) was sequenced on the Applied Biosystems SOLiD 3.5 platform to generate 50 bp reads. Sequence reads were aligned with the *Gallus gallus* reference genome (*galGal3*). More than 1 million reads were mapped for each sample. Aligned reads were extended to 100 bp in the 3′ direction. The number of reads was summed up in a 150 bp window with a step size of 10 bp along the chromosome for ChIP and WCE fractions, respectively. After normalization of total reads of the ChIP fraction against the WCE fraction, enrichment values (ChIP/WCE) were calculated as described previously (Lengronne et al., 2004) for each window.

For ChIP-qPCR, DNA samples from the WCE and ChIP fractions were sheared with the ultra sonicator, incubated with p300 antibody and purified. Putative binding site sequences were amplified with specific primers (for negative control, 5′-TCTGCATGCTGTGTGTCAAA-3′ and 5′-GCAGATC-CAAAAGCATCCAT-3′; for BS-*p63*, 5′-CAGCAGATAAGCGTGCAAG-A-3′ and 5′-GCACAGTGACTCGACAAAGG-3′; for BS-*p73*, 5′-TCACAT-GTGGTTCCCAGCTA-3′ and 5′-GTTGGAAGGCATGTGGAAGT-3′). The mean±s.d. was calculated, and a statistical analysis was performed using Student's *t*-test.

Acknowledgements

We thank Koichi Kawakami, Stephen Hughes, Toshihiko Ogura and Junichi Miyazaki for plasmids. We also thank Takayuki Suzuki, Yuji Watanabe, Yuji Yokouchi, Bau-Lin Huang, Hidenori Nishihara, Makiha Hukuda and Tomoya Itoh for technical advice; Satoru Takahashi for sharing unpublished information; and John Fallon for critical comments.

Competing interests

The authors declare no competing financial interests.

Author contributions

N.S. and M.T. designed the project. N.S. performed most of the embryological, cellular and biochemical experiments except those described below. D.S. performed some implantation experiments. M.T. built some DNA constructs. Y.K. performed

sequencing analysis. T.I. and R.N. performed computational analysis. K.K. and C.T. provided materials and advice. M.B. advised on the ChIP analysis. K.S. advised on ChIP analysis and supervised the sequencing analysis. N.S. and M.T. wrote the manuscript.

Funding
This work is supported by a Grant-in-Aid for Scientific Research on Innovative Areas [24113503 to M.T.], by the Takeda Science Foundation (M.T.) and by a Sasakawa Scientific Research Grant (N.S.).

Supplementary material
Supplementary material available online at
http://dev.biologists.org/lookup/suppl/doi:10.1242/dev.099150/-/DC1

References

Alles, A. J. and Sulik, K. K. (1989). Retinoic-acid-induced limb-reduction defects: perturbation of zones of programmed cell death as a pathogenetic mechanism. *Teratology* **40**, 163-171.
Bakri, Y., Sarrazin, S., Mayer, U. P., Tillmanns, S., Nerlov, C., Boned, A. and Sieweke, M. H. (2005). Balance of MafB and PU.1 specifies alternative macrophage or dendritic cell fate. *Blood* **105**, 2707-2716.
Bangs, F., Antonio, N., Thongnuek, P., Welten, M., Davey, M. G., Briscoe, J. and Tickle, C. (2011). Generation of mice with functional inactivation of talpid3, a gene first identified in chicken. *Development* **138**, 3261-3272.
Boardman, P. E., Sanz-Ezquerro, J., Overton, I. M., Burt, D. W., Bosch, E., Fong, W. T., Tickle, C., Brown, W. R. A., Wilson, S. A. and Hubbard, S. J. (2002). A comprehensive collection of chicken cDNAs. *Curr. Biol.* **12**, 1965-1969.
Chen, Y., Knezevic, V., Ervin, V., Hutson, R., Ward, Y. and Mackem, S. (2004). Direct interaction with Hoxd proteins reverses Gli3-repressor function to promote digit formation downstream of Shh. *Development* **131**, 2339-2347.
Crossley, P. H., Minowada, G., MacArthur, C. A. and Martin, G. R. (1996). Roles for FGF8 in the induction, initiation, and maintenance of chick limb development. *Cell* **84**, 127-136.
Das, R. M., Van Hateren, N. J., Howell, G. R., Farrell, E. R., Bangs, F. K., Porteous, V. C., Manning, E. M., McGrew, M. J., Ohyama, K., Sacco, M. A. et al. (2006). A robust system for RNA interference in the chicken using a modified microRNA operon. *Dev. Biol.* **294**, 554-563.
Deppmann, C. D., Alvania, R. S. and Taparowsky, E. J. (2006). Cross-species annotation of basic leucine zipper factor interactions: insight into the evolution of closed interaction networks. *Mol. Biol. Evol.* **23**, 1480-1492.
Dupé, V., Ghyselinck, N. B., Thomazy, V., Nagy, L., Davies, P. J. A., Chambon, P. and Mark, M. (1999). Essential roles of retinoic acid signaling in interdigital apoptosis and control of BMP-7 expression in mouse autopods. *Dev. Biol.* **208**, 30-43.
Ecevit, O., Khan, M. A. and Goss, D. J. (2010). Kinetic analysis of the interaction of b/HLH/Z transcription factors Myc, Max, and Mad with cognate DNA. *Biochemistry* **49**, 2627-2635.
Flinterman, M., Guelen, L., Ezzati-Nik, S., Killick, R., Melino, G., Tominaga, K., Mymryk, J. S., Gaken, J. and Tavassoli, M. (2005). E1A activates transcription of p73 and Noxa to induce apoptosis. *J. Biol. Chem.* **280**, 5945-5959.
Flores, E. R., Tsai, K. Y., Crowley, D., Sengupta, S., Yang, A., McKeon, F. and Jacks, T. (2002). p63 and p73 are required for p53-dependent apoptosis in response to DNA damage. *Nature* **416**, 560-564.
Francis, J. C., Radtke, F. and Logan, M. P. O. (2005). Notch1 signals through Jagged2 to regulate apoptosis in the apical ectodermal ridge of the developing limb bud. *Dev. Dyn.* **234**, 1006-1015.
Ganan, Y., Macias, D., Duterque-Coquillaud, M., Ros, M. A. and Hurle, J. M. (1996). Role of TGF beta s and BMPs as signals controlling the position of the digits and the areas of interdigital cell death in the developing chick limb autopod. *Development* **122**, 2349-2357.
Hamada, M., Nakamura, M., Tran, M. T. N., Moriguchi, T., Hong, C., Ohsumi, T., Dinh, T. T. H., Kusakabe, M., Hattori, M., Katsumata, T. et al. (2014). MafB promotes atherosclerosis by inhibiting foam-cell apoptosis. *Nat. Commun.* **5**, 3147.
Hernandez-Martinez, R., Castro-Obregon, S. and Covarrubias, L. (2009). Progressive interdigital cell death: regulation by the antagonistic interaction between fibroblast growth factor 8 and retinoic acid. *Development* **136**, 3669-3678.
Homburger, S. A. and Fekete, D. M. (1996). High efficiency gene transfer into the embryonic chicken CNS using B-subgroup retroviruses. *Dev. Dyn.* **206**, 112-120.
Hubbard, S. J., Grafham, D. V., Beattie, K. J., Overton, I. M., McLaren, S. R., Croning, M. D. R., Boardman, P. E., Bonfield, J. K., Burnside, J., Davies, R. M. et al. (2005). Transcriptome analysis for the chicken based on 19,626 finished cDNA sequences and 485,337 expressed sequence tags. *Genome Res.* **15**, 174-183.
Hughes, S. H., Greenhouse, J. J., Petropoulos, C. J. and Sutrave, P. (1987). Adaptor plasmids simplify the insertion of foreign DNA into helper-independent retroviral vectors. *J. Virol.* **61**, 3004-3012.
Kataoka, K., Fujiwara, K. T., Noda, M. and Nishizawa, M. (1994a). MafB, a new Maf family transcription activator that can associate with Maf and Fos but not with Jun. *Mol. Cell. Biol.* **14**, 7581-7591.
Kataoka, K., Noda, M. and Nishizawa, M. (1994b). Maf nuclear oncoprotein recognizes sequences related to an AP-1 site and forms heterodimers with both Fos and Jun. *Mol. Cell. Biol.* **14**, 700-712.
Kawakami, K. and Noda, T. (2004). Transposition of the Tol2 element, an Ac-like element from the Japanese medaka fish Oryzias latipes, in mouse embryonic stem cells. *Genetics* **166**, 895-899.
Kelly, L. M., Englmeier, U., Lafon, I., Sieweke, M. H. and Graf, T. (2000). MafB is an inducer of monocytic differentiation. *EMBO J.* **19**, 1987-1997.
Kouwenhoven, E. N., van Heeringen, S. J., Tena, J. J., Oti, M., Dutilh, B. E., Alonso, M. E., de la Calle-Mustienes, E., Smeenk, L., Rinne, T., Parsaulian, L. et al. (2010). Genome-wide profiling of p63 DNA-binding sites identifies an element that regulates gene expression during limb development in the 7q21 SHFM1 locus. *PLoS Genet.* **6**, e1001065.
Lecoin, L., Sii-Felice, K., Pouponnot, C., Eychène, A. and Felder-Schmittbuhl, M.-P. (2004). Comparison of maf gene expression patterns during chick embryo development. *Gene Expr. Patterns* **4**, 35-46.
Lengronne, A., Katou, Y., Mori, S., Yokobayashi, S., Kelly, G. P., Itoh, T., Watanabe, Y., Shirahige, K. and Uhlmann, F. (2004). Cohesin relocation from sites of chromosomal loading to places of convergent transcription. *Nature* **430**, 573-578.
Leventaki, V., Drakos, E., Medeiros, L. J., Lim, M. S., Elenitoba-Johnson, K. S., Claret, F. X. and Rassidakis, G. Z. (2007). NPM-ALK oncogenic kinase promotes cell-cycle progression through activation of JNK/cJun signaling in anaplastic large-cell lymphoma. *Blood* **110**, 1621-1630.
Lindsten, T. and Thompson, C. B. (2006). Cell death in the absence of Bax and Bak. *Cell Death Differ.* **13**, 1272-1276.
Lussier, M., Canoun, C., Ma, C., Sank, A. and Shuler, C. (1993). Interdigital soft tissue separation induced by retinoic acid in mouse limbs cultured in vitro. *Int. J. Dev. Biol.* **37**, 555-564.
Macias, D., Ganan, Y., Sampath, T. K., Piedra, M. E., Ros, M. A. and Hurle, J. M. (1997). Role of BMP-2 and OP-1 (BMP-7) in programmed cell death and skeletogenesis during chick limb development. *Development* **124**, 1109-1117.
Mandal, C. C., Ganapathy, S., Gorin, Y., Mahadev, K., Block, K., Abboud, H. E., Harris, S. E., Ghosh-Choudhury, G. and Ghosh-Choudhury, N. (2011). Reactive oxygen species derived from Nox4 mediate BMP2 gene transcription and osteoblast differentiation. *Biochem. J.* **433**, 393-402.
Mariani, F. V., Ahn, C. P. and Martin, G. R. (2008). Genetic evidence that FGFs have an instructive role in limb proximal-distal patterning. *Nature* **453**, 401-405.
Mechta-Grigoriou, F., Giudicelli, F., Pujades, C., Charnay, P. and Yaniv, M. (2003). c-jun regulation and function in the developing hindbrain. *Dev. Biol.* **258**, 419-431.
Melino, G., Lu, X., Gasco, M., Crook, T. and Knight, R. A. (2003). Functional regulation of p73 and p63: development and cancer. *Trends Biochem. Sci.* **28**, 663-670.
Mills, A. A., Zheng, B., Wang, X.-J., Vogel, H., Roop, D. R. and Bradley, A. (1999). p63 is a p53 homologue required for limb and epidermal morphogenesis. *Nature* **398**, 708-713.
Morgan, B. A. and Fekete, D. M. (1996). Manipulating gene expression with replication-competent retroviruses. *Methods Cell Biol.* **51**, 185-218.
Nishizawa, M., Fu, S.-L., Kataoka, K. and Vogt, P. K. (2003). Artificial oncoproteins: modified versions of the yeast bZip protein GCN4 induce cellular transformation. *Oncogene* **22**, 7931-7941.
Niwa, H., Yamamura, K.-i. and Miyazaki, J.-i. (1991). Efficient selection for high-expression transfectants with a novel eukaryotic vector. *Gene* **108**, 193-199.
Ogino, H. and Yasuda, K. (1998). Induction of lens differentiation by activation of a bZIP transcription factor, L-Maf. *Science* **280**, 115-118.
Ogura, T. (2002). In vivo electroporation: a new frontier for gene delivery and embryology. *Differentiation* **70**, 163-171.
Pyati, U. J., Gjini, E., Carbonneau, S., Lee, J.-S., Guo, F., Jette, C. A., Kelsell, D. P. and Look, A. T. (2011). p63 mediates an apoptotic response to pharmacological and disease-related ER stress in the developing epidermis. *Dev. Cell* **21**, 492-505.
Robledo, R. F., Rajan, L., Li, X. and Lufkin, T. (2002). The Dlx5 and Dlx6 homeobox genes are essential for craniofacial, axial, and appendicular skeletal development. *Genes Dev.* **16**, 1089-1101.
Rodriguez-Leon, J., Merino, R., Macias, D., Gañan, Y., Santesteban, E. and Hurle, J. M. (1999). Retinoic acid regulates programmed cell death through BMP signalling. *Nat. Cell Biol.* **1**, 125-126.
Ros, M. A., Piedra, M. E., Fallon, J. F. and Hurle, J. M. (1997). Morphogenetic potential of the chick leg interdigital mesoderm when diverted from the cell death program. *Dev. Dyn.* **208**, 406-419.

Development (2014) 141, 2885-2894 doi:10.1242/dev.099150

Salas-Vidal, E., Lomeli, H., Castro-Obregón, S., Cuervo, R., Escalante-Alcalde, D. and Covarrubias, L. (1998). Reactive oxygen species participate in the control of mouse embryonic cell death. *Exp. Cell Res.* **238**, 136-147.

Sasaki, Y., Ishida, S., Morimoto, I., Yamashita, T., Kojima, T., Kihara, C., Tanaka, T., Imai, K., Nakamura, Y. and Tokino, T. (2002). The p53 family member genes are involved in the Notch signal pathway. *J. Biol. Chem.* **277**, 719-724.

Schnabel, D., Salas-Vidal, E., Narváez, V., Sánchez-Carbente Mdel, R., Hernández-García, D., Cuervo, R. and Covarrubias, L. (2006). Expression and regulation of antioxidant enzymes in the developing limb support a function of ROS in interdigital cell death. *Dev. Biol.* **291**, 291-299.

Sen, C. K. and Packer, L. (1996). Antioxidant and redox regulation of gene transcription. *Faseb J.* **10**, 709-720.

Shaulian, E. and Karin, M. (2002). AP-1 as a regulator of cell life and death. *Nat. Cell Biol.* **4**, E131-E136.

Tang, M. K., Leung, A. K. C., Kwong, W. H., Chow, P. H., Chan, J. Y. H., Ngo-Muller, V., Li, M. and Lee, K. K. H. (2000). Bmp-4 requires the presence of the digits to initiate programmed cell death in limb interdigital tissues. *Dev. Biol.* **218**, 89-98.

Todt, W. L. and Fallon, J. F. (1986). Development of the apical ectodermal ridge in the chick leg bud and a comparison with the wing bud. *Anat. Rec.* **215**, 288-304.

Tümpel, S., Sanz-Ezquerro, J. J., Isaac, A., Eblaghie, M. C., Dobson, J. and Tickle, C. (2002). Regulation of Tbx3 expression by anteroposterior signalling in vertebrate limb development. *Dev. Biol.* **250**, 251-262.

Urasaki, A., Morvan, G. and Kawakami, K. (2006). Functional dissection of the Tol2 transposable element identified the minimal cis-sequence and a highly repetitive sequence in the subterminal region essential for transposition. *Genetics* **174**, 639-649.

Urist, M., Tanaka, T., Poyurovsky, M. V. and Prives, C. (2004). p73 induction after DNA damage is regulated by checkpoint kinases Chk1 and Chk2. *Genes Dev.* **18**, 3041-3054.

Vartanian, R., Masri, J., Martin, J., Cloninger, C., Holmes, B., Artinian, N., Funk, A., Ruegg, T. and Gera, J. (2011). AP-1 regulates cyclin D1 and c-MYC transcription in an AKT-dependent manner in response to mTOR inhibition: role of AIP4/Itch-mediated JUNB degradation. *Mol. Cancer Res.* **9**, 115-130.

Visel, A., Blow, M. J., Li, Z., Zhang, T., Akiyama, J. A., Holt, A., Plajzer-Frick, I., Shoukry, M., Wright, C., Chen, F. et al. (2009). ChIP-seq accurately predicts tissue-specific activity of enhancers. *Nature* **457**, 854-858.

Wang, C.-K. L., Omi, M., Ferrari, D., Cheng, H.-C., Lizarraga, G., Chin, H.-J., Upholt, W. B., Dealy, C. N. and Kosher, R. A. (2004). Function of BMPs in the apical ectoderm of the developing mouse limb. *Dev. Biol.* **269**, 109-122.

Wang, Z., Young, R. L., Xue, H. and Wagner, G. P. (2011). Transcriptomic analysis of avian digits reveals conserved and derived digit identities in birds. *Nature* **477**, 583-586.

Wilkinson, D. G. (1992). *In Situ Hybridization: A Practival Approach*. Oxford: IRL Press/Oxford Univeristy Press.

Yang, A., Schweitzer, R., Sun, D., Kaghad, M., Walker, N., Bronson, R. T., Tabin, C., Sharpe, A., Caput, D., Crum, C. et al. (1999). p63 is essential for regenerative proliferation in limb, craniofacial and epithelial development. *Nature* **398**, 714-718.

Yang, A., Walker, N., Bronson, R., Kaghad, M., Oosterwegel, M., Bonnin, J., Vagner, C., Bonnet, H., Dikkes, P., Sharpe, A. et al. (2000). p73-deficient mice have neurological, pheromonal and inflammatory defects but lack spontaneous tumours. *Nature* **404**, 99-103.

Yao, J.-Y., Pao, C.-C. and Chen, J.-K. (2010). Transcriptional activity of TAp63 promoter is regulated by c-jun. *J. Cell. Physiol.* **225**, 898-904.

Yokouchi, Y., Sakiyama, J., Kameda, T., Iba, H., Suzuki, A., Ueno, N. and Kuroiwa, A. (1996). BMP-2/-4 mediate programmed cell death in chicken limb buds. *Development* **122**, 3725-3734.

Yokoyama, S., Ito, Y., Ueno-Kudoh, H., Shimizu, H., Uchibe, K., Albini, S., Mitsuoka, K., Miyaki, S., Kiso, M., Nagai, A. et al. (2009). A systems approach reveals that the myogenesis genome network is regulated by the transcriptional repressor RP58. *Dev. Cell* **17**, 836-848.

Zheng, T. S., Hunot, S., Kuida, K. and Flavell, R. A. (1999). Caspase knockouts: matters of life and death. *Cell Death Differ.* **6**, 1043-1053.

Zou, H. and Niswander, L. (1996). Requirement for BMP signaling in interdigital apoptosis and scale formation. *Science* **272**, 738-741.

Zuzarte-Luis, V. and Hurle, J. M. (2002). Programmed cell death in the developing limb. *Int. J. Dev. Biol.* **46**, 871-876.